REVIEW ARTICLE

Construction and Analysis of lncRNA-miRNA-mRNA ceRNA Network Identify an Eight-Gene Signature as a Potential Prognostic Factor in Kidney Renal Papillary Cell Carcinoma (KIRP)

Lei Yang, MD; Tian-Jiao Ma, MD; Yu-Bai Zhang, MD; He Wang, MD; Rui-Hua An, PhD

ABSTRACT

Aims • This study was conducted to establish the potential competing endogeneous RNA (ceRNA) network for predicting prognoses in kidney papillary renal cell carcinoma (KIRP) and explore novel therapeutic targets.

Methods • The edgeR package in R was used to determine differentially expressed messenger RNAs (mRNAs), long non-coding RNAs (lncRNAs) and microRNAs (miRNAs), based on data from The Cancer Gene Atlas Program (TCGA) and the Genotype Expression (GTEx) databases. Weighted gene co-expression network analysis (WGCNA) was performed to filter out the mRNAs or lncRNAs that were strongly related to KIRP. The miRNAs that possibly sponged by differentially expressed RNAs lncRNAs (DElncRNAs) were screened using miRcode. Starbase, miRDB, and TargetScan sets were utilized to predict target mRNAs to corresponding miRNAs. LASSO and multivariate Cox regression analyses were applied for the determination of potential prognostic significance. Finally, the lncRNA-miRNA-mRNA ceRNA network was constructed.

Results • A total of 1739 DEmRNAs and 1599 DElncRNAs were identified in KIRP. WGCNA analysis suggested that DEmRNAs in the blue module and DElncRNAs in the turquoise module were closely correlated with KIRP. An 8-gene signature was constructed, which had prognostic significance and predictive value in KIRP. Of note, a lncRNA-miRNA-mRNA ceRNA network (including 18 lncRNAs, 5 miRNAs, and 7 mRNAs) was established.

Conclusion • This investigation constructed a new lncRNA-miRNA-mRNA ceRNA network, and proposed some genes that may be novel targets, as well as a theoretical basis for the treatment of patients with KIRP. (*Altern Ther Health Med.* 2022;28(6):42-51)

Lei Yang, MD; Bai Zhang, MD; Rui-Hua An, PhD; Department of Urinary Surgery, The First Affiliated Hospital of Harbin Medical University, Harbin, Heilongjiang, China. **Tian-Jiao Ma, MD,** Department of Cardiology, Heilongjiang Provincial Hospital, Harbin, Heilongjiang, China. **He Wang, MD,** Department of Urinary Surgery, Harbin First Hospital, Harbin, Heilongjiang, China.

Corresponding author: Rui-Hua An, PhD
E-mail: ruihuaan@126.com

INTRODUCTION

Renal cell carcinoma (RCC) is the most common kidney cancer, constituting 3% of all adult tumors, and primarily divided into 3 histologic subtypes: clear cell renal cell carcinoma (ccRCC; 70%), kidney renal papillary cell carcinoma (KIRP; 10%-15 %) and chromophobe cell carcinoma (5%).[1,2] KIRP was formally admitted as a distinct entity in the Heidelberg Classification of Renal Cell Tumours, including type 1 and type 2.[3] Type 1 accounts for 35% of KIRP with a >85% 5-year survival rate, and features single layered small cells with little cytoplasm, while type 2 represents 20% of KIRP, has an approximately 45% 5-year survival rate and is characterized by large pseudostratified cells and eosinophilic cytoplasm.[4,5] Since it is difficult to diagnose in the early stages, most patients with KIRP are diagnosed with metastatic disease or when KIRP has reached an advanced stage. At present, surgical resection is the preferred therapeutic strategy, despite the fact that nearly 40% of patients with KIRP who undergo surgery relapse.[6] Thus, identifying potential prognostic biomarkers and therapeutic targets for KIRP is of great importance.

With the development of high-throughput sequencing technology, human genes have been mainly classified into 2 groups: protein-coding messenger RNAs (mRNAs) and non-coding RNAs (ncRNAs).[7] In the human genome, ncRNAs comprise the majority of all transcribed genes, of which encoding protein does not exceed 2%.[8] Nevertheless, the high percentage of ncRNAs in the genome still attracts a tremendous amount of interest by scientists, and emerging evidence suggests that different ncRNAs play important roles in multiple disorders, including cancer.[9-11]

ncRNAs consist of ribosomal RNAs (rRNAs), short ncRNAs (miRNAs), small interfering RNAs (siRNAs), transfer RNAs (tRNAs), small nucleolar RNAs (snoRNAs) and piwi-interacting (piRNAs) and long ncRNAs (lncRNAs). Of these, miRNAs and lncRNAs have been considered hot spots for tumorigenesis.[12,13] miRNAs are <25 nucleotides in length and induce transcript degradation or translational suppression through binding with miRNA response elements, thereby having carcinogenic or tumor inhibitory effects.[14-16] LncRNAs are relatively long (approximately ≥200 nucleotides) ncRNAs. An increasing number of studies have determined that lncRNAs have transcriptional and post-transcriptional regulatory influence.[17] In the competing endogenous RNA (ceRNA) hypothesis, first proposed by Salmena, et al. in 2011, lncRNAs can act as ceRNAs and interact with mRNAs by competitively titrating their common miRNAs.[18]

Recently, a great many studies have identified several prognostic and therapeutic markers by using ceRNA interaction. For example, LINC01133 has been determined to be a ceRNA and suppresses the progression of gastric cancer via sponging miR-106a-3p and regulating adenomatous polyposis coli (APC) expression.[19] Kong, et al. suggested that lncRNA-CDC6 stimulates breast cancer development and serves as a ceRNA to target CDC6 via sponging miR-215.[20] LncRNA UICLM-miR-215-ZEB2 coordinates liver metastasis in patients with colorectal cancer.[21] However, prior investigations have only emphasized the mechanism of the single lncRNA-miRNA-mRNA axis, and there are few reports concerning the ceRNA network in KIRP.

Thus, in our study we carried out this exploration and aimed to construct an lncRNA-miRNA-mRNAs ceRNA network using weighted-gene co-expression network analysis (WGCNA) and LASSO Cox analyses based on the TCGA and GTEx databases. This study will assist in the determination of novel targets for the prediction of the prognosis in patients with KIRP.

MATERIALS AND METHODS

Data Sources and Pre-processing

RNA-Seq expression profiles and clinical data for KIRP were retrieved from The Cancer Genome Atlas (TCGAT) database (https://portal.gdc.cancer.gov/), which included 322 samples; gene expression profile data of a total of 89 normal kidney tissue samples were downloaded from the Genotype-Tissue Expression (GTRX) portal (https://gtexportal.org/).

The data were mainly analyzed by the program code written in the Perl and R language package, and the detailed steps were as follows:

(1) **Extraction of the matrix file from raw data**. Perl language package was used to process and merge all the RNA-Seq profiles from 411 clinical samples and extracted the matrix file.
(2) **Transformation gene name**. By accessing the Ensembl genome browser (www.ensembl.org/index.html), the corresponding file of Ensembl ID and gene names (Homo_sapiens.GRCh38.89.chr.gtf) were obtained. After converting the Ensemble ID into the corresponding gene using Perl, we obtained the gene expression profiles for all samples.

Identification of Differentially Expressed mRNAs (DEmRNAs) and lncRNAs (DElncRNAs)

EdgeR in R software, which can be accessed at https://bioconductor.org/packages/release/bioc/html/edgeR.html, was utilized to screen DEmRNAs and DElncRNAs based on the data obtained from the TCGA and GTEx databases. The 411 samples were divided into 2 groups: the tumor group and the normal group. The log fold change (FC)≥2 and false discovery rate (FDR) <.05 were considered the screening conditions.

Functional Annotation of DEmRNAs

To further understand the biological function of DEmRNAs, Gene Ontology (GO), Kyoto Encyclopedia of Genes and Genomes (KEGG), and Gene Set Enrichment Analysis (GSEA) were performed.

WGCNA for DEmRNAs and DElncRNAs

WGCNA is a bioinformatics method, which was used on tumor samples using the R package and employed to construct co-expression. DEmRNAs and DElncRNAs expression values were presented in the form of log2 (TPM+0.001). The optimal soft threshold was determined by selecting the least value for R^2 index >0.75. The correlation of all paired genes was determined by Pearson correlation analysis. Then, based on the soft threshold power, the co-expression matrix was converted into the adjacent matrix. The scale-free co-expression network was ensured by the soft threshold. Genes with high correlations were clustered into the same module. For DEmRNAs, the soft threshold was 2 ($\beta = 2$), the minimal module size was 25 and the dendrogram cut height was 0.25. For DElncRNAs, 25 was set as minModuleSize with $\beta = 3$ and MEDissThres was 0.25. Modules ($r > 0.25$) were merged.

Prediction of Possible miRNAs and Prognostic riskScore model

miRcode (http://www.mircode.org/) was used to detect the interactions between lncRNAs and miRNAs. Starbase (http://starbase.sysu.edu.cn/), miRDB (http://www.mirdb.org/), and TargetScan (http://www.targetscan.org/) were employed for the identification of the miRNAs-mRNAs correlations. To achieve the lncRNAs-miRNAs, miRcode was first utilized to predict the miRNAs generated by 1293 lncRNAs in the turquoise module. Then, the top 400 highly expressed miRNAs in TCGA-KIRP were filtered and intersected with the miRNAs predicted by miRcode. The common mRNAs were obtained by intersecting the putative target mRNAs of miRNAs (Starbase, miRDB and TargetScan), the mRNAs in the blue module and DEmRNAs (upregulated and downregulated mRNAs) screened with edgeR (TCGA portal).

Figure 1. Volcano plots representing the expression of differentially expressed (A) mRNAs (DEmRNAs) and (B) lncRNAs (DElncRNAs). Red denotes upregulated mRNAs or lncRNAs, while blue denotes downregulated mRNAs or lncRNAs.

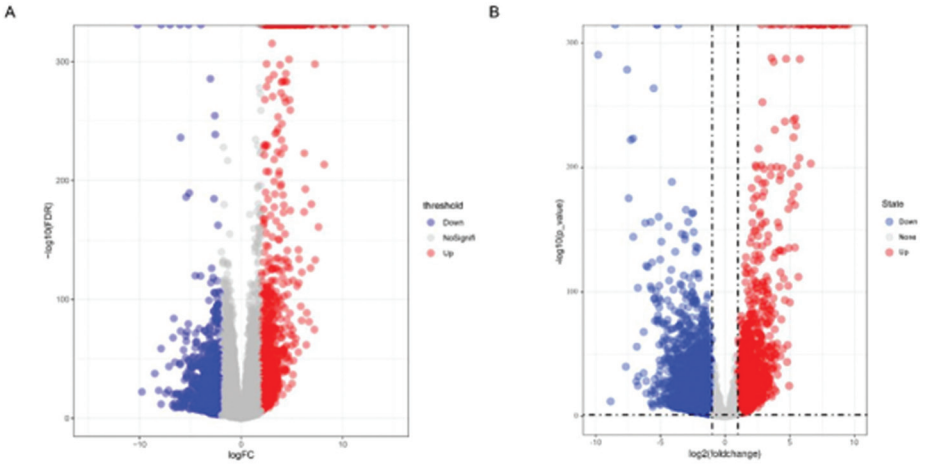

Abbreviations: DElncRNA, differentially expressed long non-coding RNA; DEmRNA, differentially expressed messenger RNA; lncRNA, long non-coding RNA; mRNA, messenger RNA.

Total common genes were assessed with univariate Cox regression analysis, and then LASSO regression analysis was performed to select genes with a *P* value <.01. The most prominent 8 genes were identified using multivariate Cox regression analysis, and weighted by their corresponding regression coefficients. The riskScore formula was:

$$\text{risk score} = (\text{expr}_{\text{gene1}} * \text{coefficient}_{\text{gene1}}) + (\text{expr}_{\text{gene2}} 8 * \text{coefficient}_{\text{gene2}}) + \ldots + (\text{expr}_{\text{genen}} * \text{coefficient}_{\text{genen}})$$

According to the median risk score, patients were classified into either the low- or high-risk group. The predictive potential of the identified signature was evaluated using a receiver operating characteristic (ROC) curve in the R package, whereas the survival differences between the high-risk and low-risk groups were assessed using the Kaplan-Meier method with the log-rank test.

Construction of the lncRNA-miRNA-mRNA ceRNA Network

The optimal potential miRNAs regulating 8 key genes were determined with the overlapping miRNAs predicted by Starbase, miRDB, and TargetScan sets. Possible lncRNAs were identified with miRcode, which should be included in the turquoise module and logFC>4. The correlations between the identified mRNAs and lncRNAs were validated with Pearson correlation analysis. On the basis of interactions between miRNA-lncRNA and miRNA-mRNA, an lncRNA-miRNA-mRNA ceRNA network was constructed.

RESULTS

DElncRNAs and DEmRNAs in KIRP

RNA-Seq expression profiles in patients with KIRP were obtained from the TCGA and GTEx portals and analyzed using the edgeR package in R. With the criteria of logFC| ≥2 and FDR <.05, a total of 1739 DEmRNAs (850 upregulated mRNAs and 889 downregulated mRNAs) and 1599 DElncRNAs (479 upregulated lncRNAs and 1120 downregulated lncRNAs) were sorted out. The volcano plots are shown in Figure 1A (for DEmRNAs) and Figure 1B (for DElncRNAs).

GO, KEGG and GSEA Analyses of DEmRNAs

In order to explore the potential functions of DEmRNAs in KIRP, all DEmRNAs were subjected to Gene Ontology (GO), Kyoto Encyclopedia of Genes and Genomes (KEGG) and Gene Set Enrichment Analysis (GSEA) analyses. As shown in Figure 2A, the results were divided into 3 parts: biological process (BP), cellular components (CC) and molecular function (MF), and the top 30 GO terms were filtered for upregulated mRNAs. Kidney development, calcium ion homeostasis and renal system development were considered the top 3 BP items; hemoglobin complex, blood microparticles, and sarcomere were regarded as the top CC items; and the top 3 MF items included serine-type peptidase activity, hydrolase activity, acting on acid phosphorus-nitrogen bonds and serine hydrolase activity.

The GO items enriched by the downregulated mRNAs are shown in Figure 2B. The results of the KEGG analyses revealed that the upregulated mRNAs were mainly enriched in protein digestion and absorption, pancreatic secretion, neuroactive ligand-receptor interaction pathway calcium signaling pathway, etc. (Figure 2C), while the downregulated mRNAs were enriched in viral protein interaction with cytokine and cytokine receptor pathway, neuroactive ligand-receptor interaction pathway, etc. (Figure 2D). GSEA results indicated that the JAK-STAT signaling pathway, pancreatic secretion, protein digestion and absorption, and Wnt signaling pathway were promoted by upregulated mRNAs,

Figure 2. GO and KEGG analyses were performed for DEmRNAs using the DAVID database. (A) The results of GO analyses of upregulated mRNAs. The horizontal axis indicates the number of genes enriched in GO items, and the vertical axis indicates different GO items divided into biological process (BP), cellular component (CC) and molecular function (MF). (B) The results of GO analyses of downregulated mRNAs. (C) The results of KEGG analyses of upregulated mRNAs. (D) The results of KEGG analyses of downregulated mRNAs.

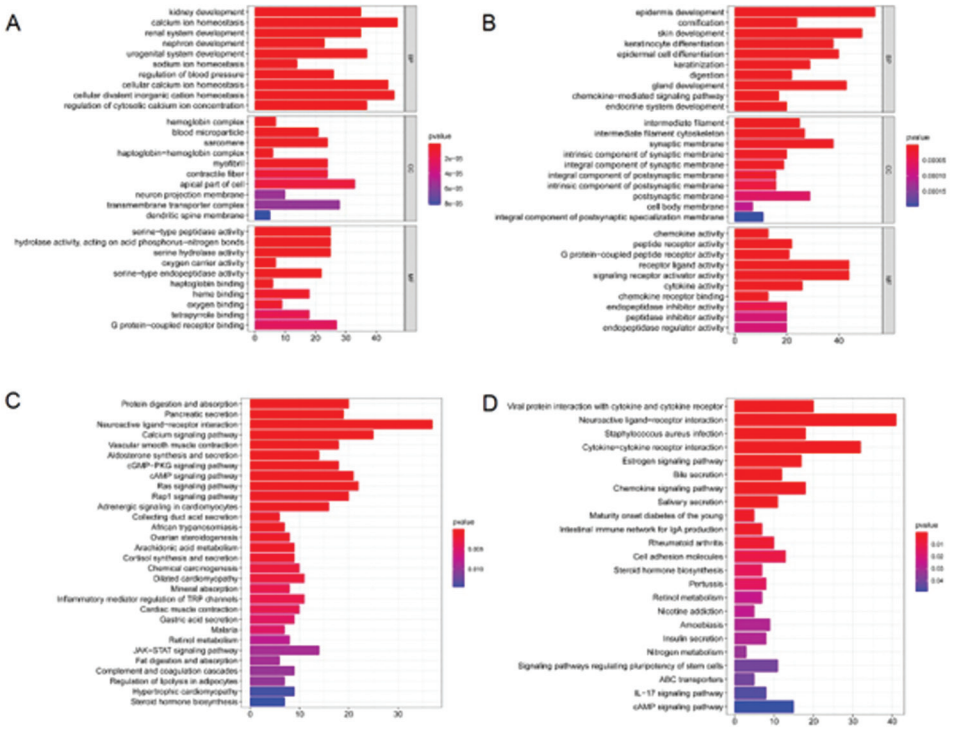

Abbreviations: BP, biological processes; CC, cellular component; DAVID, Database for Annotation, Visualization, and Integrated Discovery; DEmRNA, differentially expressed messenger RNA; GO, Gene Ontology; KEGG, Kyoto Encyclopedia of Genes and Genomes; MF, molecular function; mRNA, messengerRNA.

Figure 3. GSEA for upregulated mRNAs (A) and downregulated mRNAs (B).

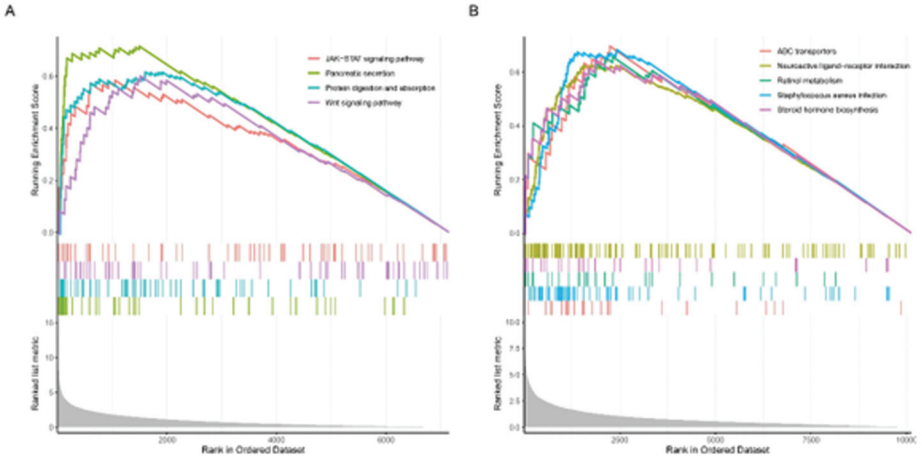

Abbreviations: GSEA, Gene Set Enrichment Analysis; mRNA, messenger RNA.

while ABC transporters, neuroactive ligand-receptor interaction, retinol metabolism, staphylococcus aureus infection and steroid hormone biosynthesis were stimulated by downregulated mRNAs (Figures 3A and 3B).

WGCNA for DEmRNAs

The genes most highly related to KIRP were analyzed by WGCNA. The adjacency matrix was defined with a 2 soft threshold power and miniModuleSize 25 (Figure 4A). The

Figure 4. WGCNA analysis for the identification of KIRP-related mRNA modules. (A) Network topology for different soft threshold powers; the scale-free topology could be obtained when the soft threshold power was 2. (B) Gene dendrogram and module colors. (C) Heatmap of topological overlap in selected genes. (D) Heatmaps of the relevance between eigengene and KIRP.

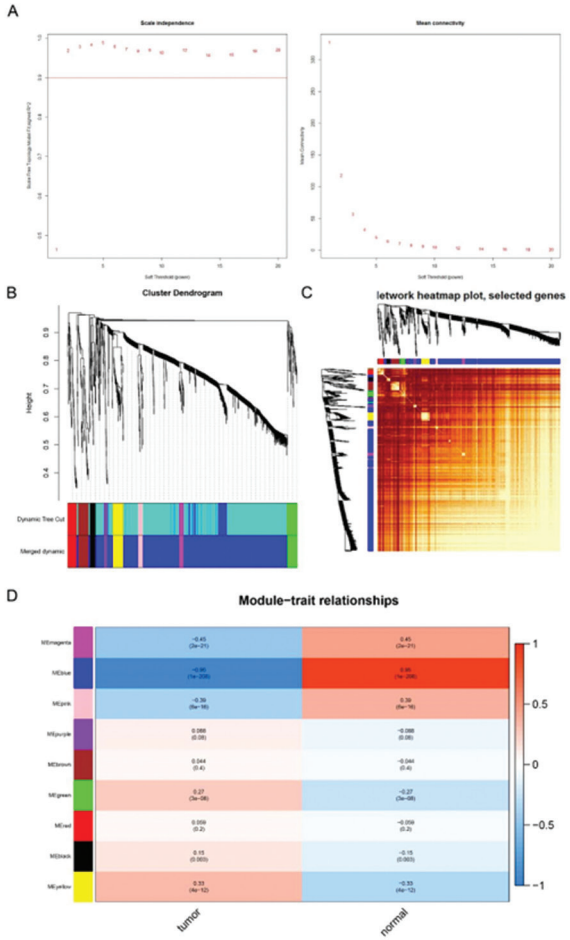

Abbreviations: KIRP, kidney renal papillary cell carcinoma; mRNA, messenger RNA; WGCNA, Weighted Gene Co-expression Network Analysis.

MEDissThres was 0.25, suggesting that the modules whose eigengenes were related more than 0.75 were merged (Figure 4B). As seen in Figure 4C, the topological overlap plot manifested that genes in modules possessed a high correlation with each other. The blue module was most strongly correlated with KIRP, with a correlation coefficient of 0.95 (Figure 4D). The blue module contained 1295 mRNAs, and further functional enrichment analysis showed that these genes were highly enriched in calcium ion homeostasis, synaptic membrane, receptor ligand activity, neuroactive ligand-receptor interaction, cytokine-cytokine receptor interaction, cAMP signaling pathway, etc. (Figures 5A and 5B). The interactions between 1295 mRNAs and BP are shown in Figure 5C.

Figure 5. GO and KEGG enrichment analyses of genes included in the blue module. (A) Bubble plots of BP, cellular components, and molecular function (MF). (B) Bubble plot of enriched KEGG pathways. (C) Network for the interaction between 1295 mRNAs and BP.

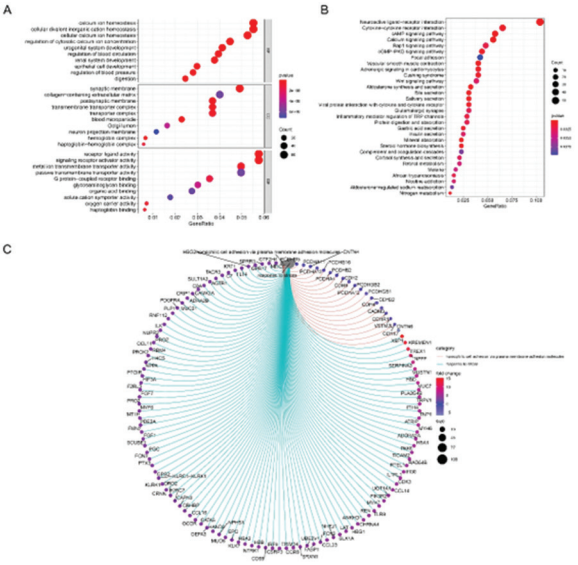

Abbreviations: BP, biological processes; CC, cellular component; GO, Gene Ontology database; KEGG, Kyoto Encyclopedia of Genes and Genomes; MF, molecular function; mRNA, messenger RNA.

Figure 6. WGCNA analysis for the identification of KIRP-associated lncRNA modules. (A) Graphs of soft threshold power and scale-free topology model; 3 was selected as the optimal soft threshold power. (B) Hierarchical clustering dendrogram of identified co-expressed lncRNAs in modules in KIRP. (C) Analysis of correlations between lncRNAs in modules and KIRP tumor or normal samples.

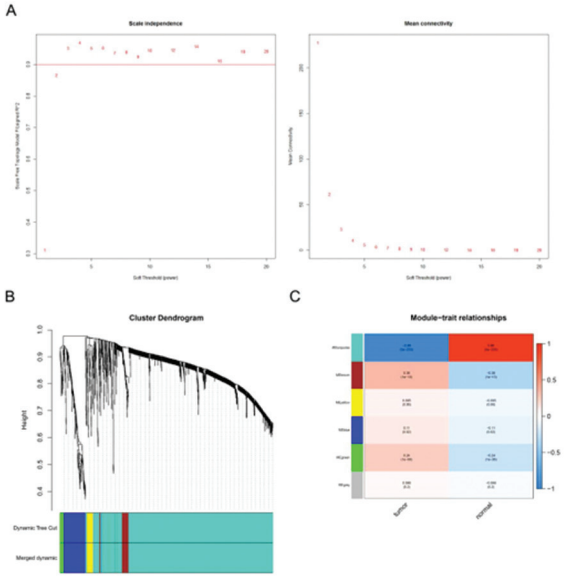

Abbreviations: KIRP, kidney renal papillary cell carcinoma; lncRNAs, long non-coding RNA.

Figure 7. Prediction of target mRNAs to corresponding miRNAs. (A) Venn graph of predicted target mRNAs, DEmRNAs based on TCGA (upregulated and downregulated mRNAs), and mRNAs in WGCNA blue module. (B) A total of 113 upregulated mRNAs and 107 downregualted mRNAs were recognized at the intersection of predicted target mRNAs, DEmRNAs, and mRNAs in the blue module. (C) Heatmap of the identified 220 genes. *Predict* = the predicted target mRNAs; *diff-up* = the upregulated differential mRNAs; *diff-down* = the downregulated differential mRNAs; *WGCNA* = mRNAs in WGCNA blue module.

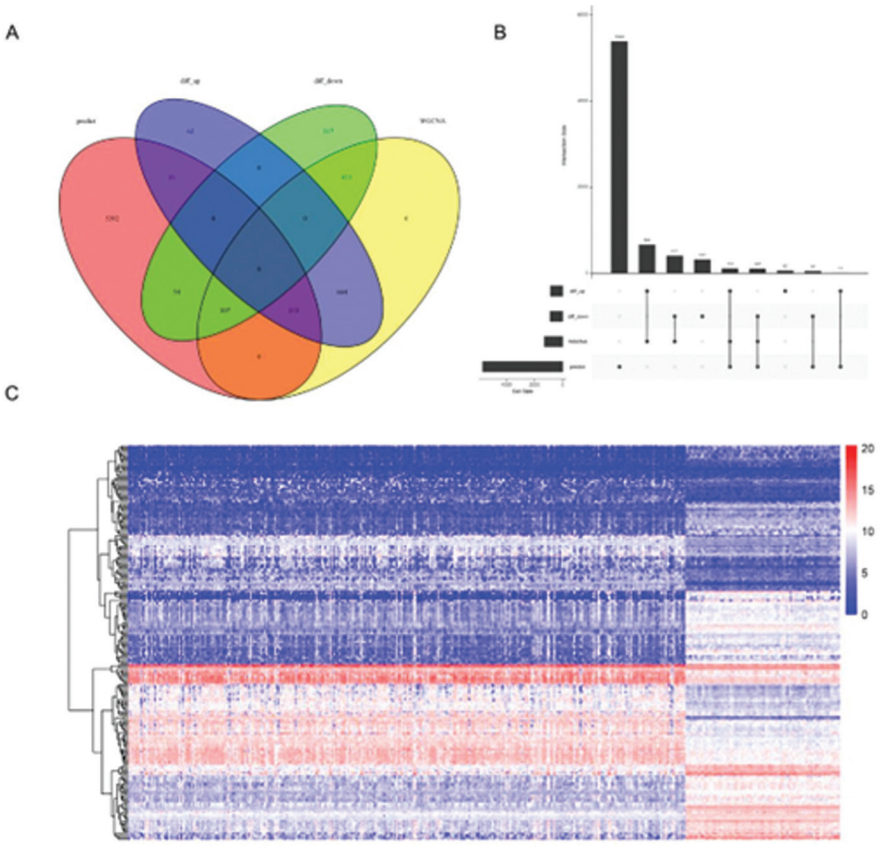

Abbreviations: DEmRNAs, differentially expressed messenger RNA; mRNA, messenger RNA; miRNA, microRNA; WGCNA, Weighted Gene Co-expression Network Analysis.

WGCNA for DElncRNAs

Next, we performed WGCNA analysis on DElncRNAs using R package and selected soft threshold power $\beta = 3$ to establish a scale-free network (Figure 6A). The minModuleSize 25 was used to determine co-expressed lncRNAs (Figure 6B). The correlation coefficients between each co-expressed gene module and normal or tumor samples are shown in **Figure 6C**. The turquoise module had the highest correlation with KIRP, with a correlation coefficient of 0.96.

Identification of the Prognostic Signature

To identify the potential miRNAs sponged by lncRNAs, we selected 1293 lncRNAs in the turquoise module that had the highest correlation with KIRP. miRcode was used to predict the miRNAs generated by 1293 lncRNAs, and thereby determined the association of lncRNA-miRcode-miRNAs. Meanwhile, we filtered the top 400 highly expressed miRNAs in KIRP based on the TCGA database to overlap the miRNAs predicted by miRcode, and finally obtained common putative miRNAs. Using Starbase, miRDB and TargetScan sets, the possible target mRNAs corresponding to miRNAs were sorted out. Subsequently, the predicted mRNAs, the mRNAs in the blue module, and the DEmRNAs (upregulated and downregulated mRNAs) obtained by edgeR package in R were intersected to filter common target mRNAs. The results showed that a total of 107 downregulated mRNAs and 113 upregulated mRNAs were obtained (Figure 7A and B). Heatmap plot of a total of 220 mRNAs is seen in Figure 7C.

Next, 220 mRNAs were analyzed by univaritate Cox regression analysis. LASSO Cox regression analysis was conducted to select mRNAs with significant prognostic value from 38 mRNAs with a $P > .01$ determined using univaritate Cox regression analysis. Results of LASSO Cox regression analysis are shown in Figure 8A. According to multivariate Cox regression analysis, a total of 8 genes were determined to establish a prognostic signature, including CCDC117, CDT1, CYP11B1, EN2, FAM26E, MS4A1, NXPH4, and PI15 (Figure

Figure 8. Screening of potential prognostic genes using the LASSO model and multivariate Cox regression analysis. (A) The distribution of every lambda and CI in LASSO Cox regression model. (B) Forest plot of hazard ratios for survival in patients with KIRP.

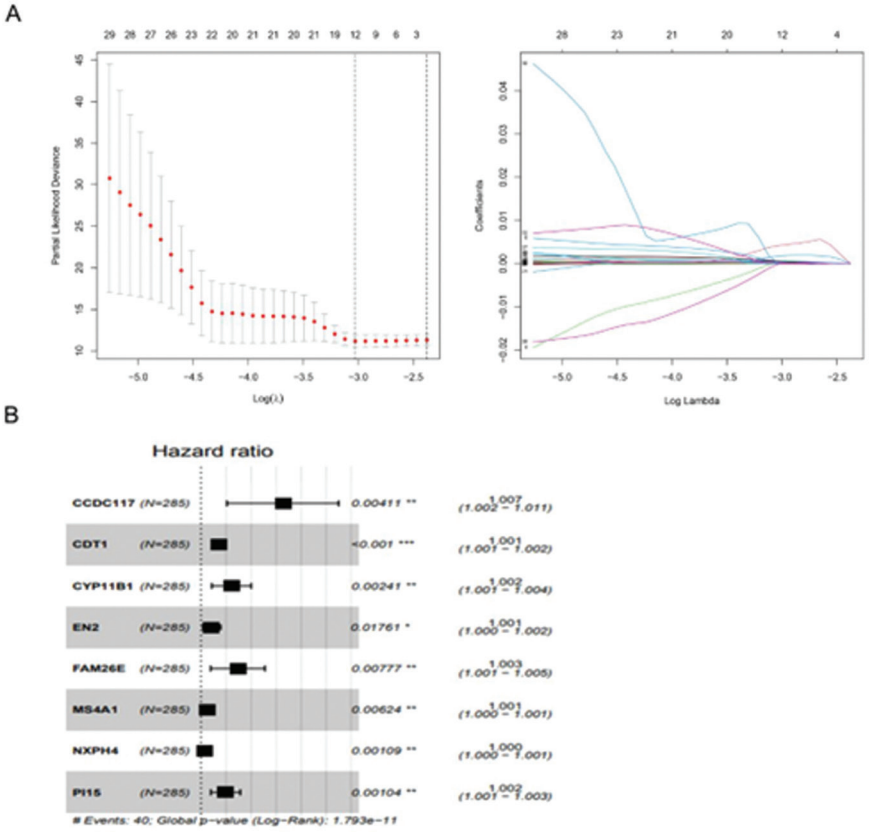

Abbreviations: CI, confidence interval; KIRP, kidney renal papillary cell carcinoma.

Figure 9. Identification of an 8-gene signature in KIRP. (A) Distribution of the risk scores. (B) Overall survival of patients with KIRP with increasing risk scores. (C) Expression profiles of 8 mRNAs. (D) Overall survival curve of patients with KIRP in the high- and low-risk groups, plotted via the Kaplan-Meier method with log-rank test. (E) ROC curve of the 8-gene signature.

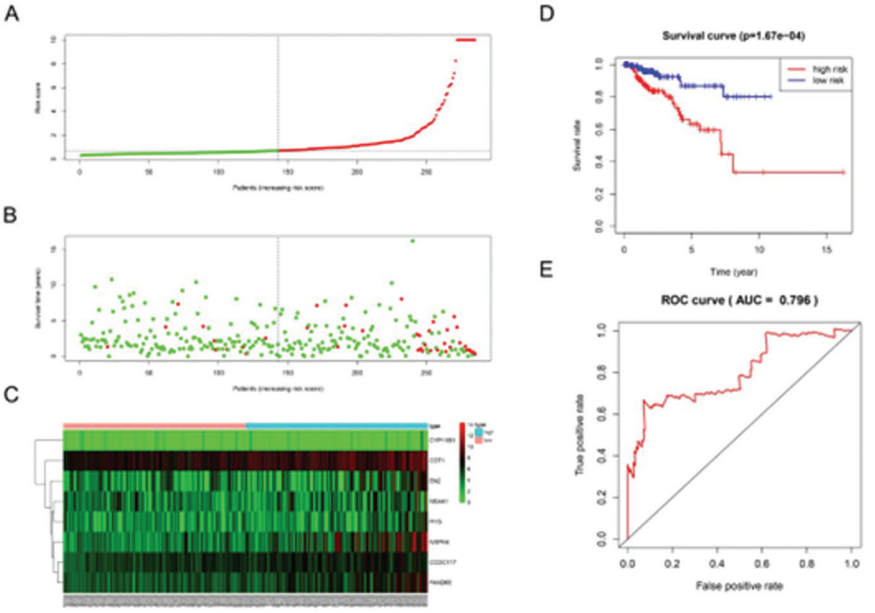

Abbreviations: KIRP, kidney renal papillary cell carcinoma; mRNA, messenger RNA; ROC, receiving operating characteristic.

Figure 10. LncRNA-miRNA-mRNAs ceRNA network. Blue round represents lncRNAs, red square represents miRNAs, and green hexagon represents mRNAs.

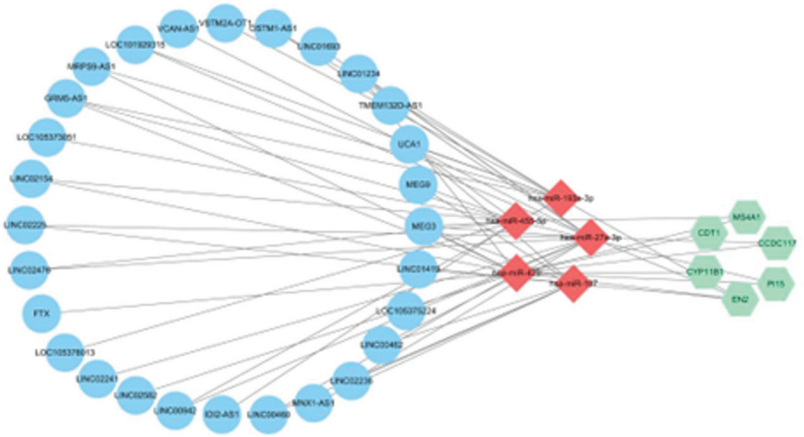

Abbreviations: ceRNA, competing endogenous RNA; lncRNA, long non-coding mRNA; mRNA, messenger RNA.

Supplementary Figure S1. Relevance of lncRNAs, miRNAs and mRNAs. (A) Intersection between 5 miRNAs and 7 mRNAs. (B) Intersection between 5 miRNAs and 18 lncRNAs. (C) Pearson correlation analysis was performed to validate the association between 7 mRNAs and 18 lncRNAs

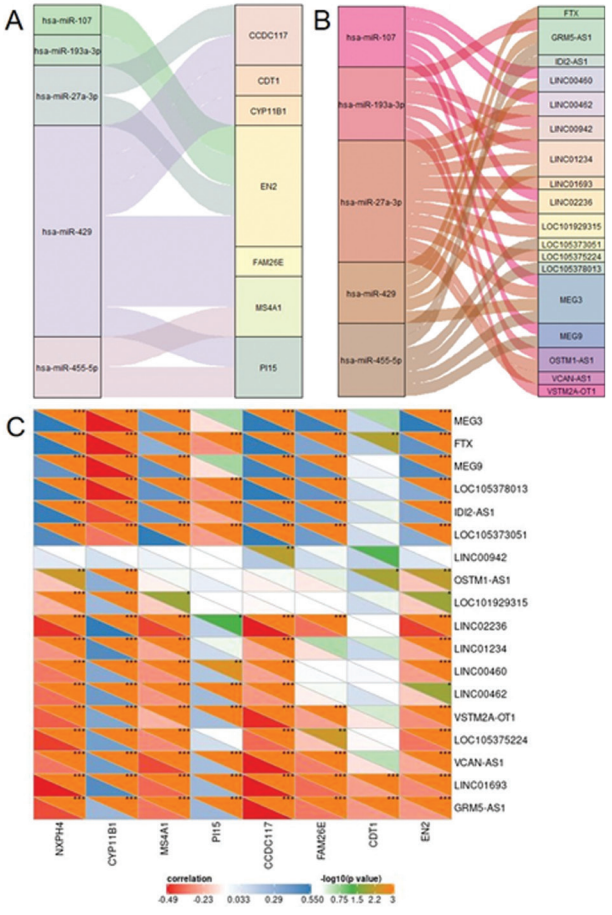

Abbreviations: lncRNA, long non-coding RNA; mRNA, messenger RNA; miRNA, microRNA.

8B). The risk score of this 8-gene signature was calculated with the following formula:

Risk Score = (0.0065*CCDC117)+(CDT1*0.0014)+(CYP11B1*0.0024) + (EN2*0.0008)+(FAM26E*0.0029)+(MS4A1*0.0005)+(NXPH4*0.0003) + (PI15*0.0019)

Together with the increased risk score, the survival rate in patients with KIRP showed a tendency to decrease (Figure 9A, 9B, and 9C). The high-risk and low-risk groups were divided on the basis of the median value of the risk scores. Kaplan-Meier analysis revealed that the overall survival rate in the high-risk group was lower than in the low-risk group (Figure 9D). The area under the curve (AUC) for overall survival was 0.796, which indicated that this 8-gene signature had significant predictive value (Figure 9E).

The LncRNA-miRNA-mRNA ceRNA network

According to the steps detailed in the MATERIALS AND METHODS section, the lncRNA-miRNA-mRNA ceRNA network was constructed, containing 18 lncRNAs, 5 miRNAs, and 7 mRNAs (Figure 10). The gene NXPH4 was removed since it had no common miRNAs with other genes (Supplementary Figure S1 A). The corresponding association between miRNAs and lncRNAs is shown in Supplementary Figure S1 B. The association between the 7 mRNAs and 18 lncRNAs was validated with Pearson correlation analysis (Supplementary Figure S1 C).

DISCUSSION

KIRP is a major subtype of RCC, and a type of refractory malignancy treated with the current therapeutic options.[22] The lack of efficacious diagnostic and prognostic markers aggravates the condition of patients with KIRP.[23] Therefore, in order to improve outcomes in patients with KIRP, exploration of the mechanism involved in KIRP progression

and identification of KIRP-associated prognostic biomarkers is urgently needed. The ceRNA hypothesis presents a new regulatory mechanism between ncRNAs and coding RNAs, which is modulated by lncRNAs (which function as miRNAs' sponges).[24] Recently, this hypothesis has received extensive attention in tumorigenesis and strong associations have been validated between ceRNA activity and the progression of various cancers.[25] Some publications have determined the ceRNA in RCC; Chen, et al. demonstrated that LINC00461, functioning as a ceRNA for miR-942, regulates the survival time of patients with RCC.[26] Yang, et al. identified 6 potential lncRNAs as prognostic biomarkers involved in ceRNA in ccRCC, but did not consider the role of miRNAs or mRNAs.[27] The importance of lncRNAs was determined in a previous study, which revealed that lncRNAs might exert crucial effects in the management of KIRP.[23] In addition, 3 other ceRNA networks have been constructed, highlighting the specific and significant role of ceRNA activity in KIRP.[28-30]

Likewise, in our study, on the basis of the theory of a ceRNA network, we established an lncRNA-miRNA-mRNA ceRNA network (including 18 lncRNAs, 5 miRNAs and 7 mRNAs) and identified an 8-gene prognostic signature. Compared with the 3 prior studies, we integrated the most clinical samples, no longer limited to the TCGA database, and also added analysis of the normal samples from the GTEx database. The establishment of a ceRNA network did not depend on Cytoscape software, but identified differentially expressed molecules via miRcode, StarBase, miRDB, TargetScan sets and Pearson's correlation analysis.

In summary, we identified an lncRNA-miRNA-mRNA ceRNA network, laying a foundation for further understanding of the effects of a ceRNA network on KIRP progression and providing more alternatives for KIRP treatment.

In the identified 8-gene signature, protein chromatin licensing and DNA replication factor 1 (CDT1) is decreased during the cell cycle, whereas these are overexpressed in cancer-derived cell lines.[31] Overexpression of CDT1 could facilitate tumorigenesis and be involved in DNA replication.[32,33] Human cytochrome P450 11B1 (CYP11B1) is a type of cytochrome P450 enzyme that is implicated in the human steroidogenesis. Fan, et al. pointed out that CYP11B1, a member of the CYP11 family, may participate in steroid hormone-related cancers.[34] Engrailed-2 (EN2) is considered a homeobox protein, and only expressed in human kidney tubular epithelial cells and adult neurons; EN2 has been reported to play an oncogenic role in ccRCC.[35] Membrane Spanning 4-Domains A1 (MS4A1) is dysregulated in asbestos-related lung cancer, indicating that MS4A1 may be a potential cancer-related protein.[36] Peptidase inhibitor 15 (PI15) is initially purified from human T98G cells as a trypsin inhibitor. PI15 has been found in multiple carcinomas, including cholangiocarcinoma, hepatocellular carcinoma and gastric carcinoma.[37,38] Moreover, based on the risk score of the 8-gene signature, the low-risk group had higher survival rates compared with the high-risk group. The ROC curve revealed that this signature had a predictive power (AUC = 0.796). Collectively, all data revealed the significance of this 8-gene signature in KIRP.

In addition, we analyzed the DEmRNAs using GO, KEGG and GSEA analyses and found that some annotated pathways, such as the JAK-STAT and Wnt signaling pathways, have been proven to be related to tumors.[39,40] After WGCNA analysis, we further estimated the functions and pathways in which the DEmRNAs of the blue module are implicated. All results showed that these mRNAs were closely related to renal system development and several signaling pathways involved in KIRP development.

Although our research has adopted the largest clinical sample data possible (TCGA and GTEx databases), longer follow-up is still required to further validate our results. In addition, future research should be performed to identify the hub genes of the lncRNA-miRNA-mRNA ceRNA network and determine the corresponding biological effects.

CONCLUSION

We constructed an lncRNA-miRNA-mRNA ceRNA network and identified an 8-gene signature by analyzing the clinical samples retrieved from TCGA and GTEx databases, which sheds new light on effective therapeutic strategies in KIRP.

CONFLICT OF INTEREST

None.

FUNDING

None.

REFERENCES

1. Znaor A, Lortet-Tieulent J, Laversanne M, Jemal A, Bray F. International variations and trends in renal cell carcinoma incidence and mortality. *Eur Urol*. 2015;67:519-530.
2. Gao Z, Zhang D, Duan Y, et al. A five-gene signature predicts overall survival of patients with papillary renal cell carcinoma. *PLoS One*. 2019;14:e0211491.
3. Kovacs G, Akhtar M, Beckwith BJ, et al. The Heidelberg classification of renal cell tumours. *J Pathol*. 1997;183:131-133.
4. Delahunt B, Eble JN. Papillary renal cell carcinoma: a clinicopathologic and immunohistochemical study of 105 tumors. *Mod Pathol*. 1997;10:53744.
5. Chen Q, Cheng L, Li Q. The molecular characterization and therapeutic strategies of papillary renal cell carcinoma. *Expert Rev Anticancer Ther*. 2019;19:169-175.
6. Courthod G, Tucci M, Di Maio M, Scagliotti GV. Papillary renal cell carcinoma: A review of the current therapeutic landscape. *Crit Rev Oncol Hematol*. 2015;96:100-112.
7. Chan JJ, Tay Y. Noncoding RNA: RNA regulatory networks in cancer. *Int J Mol Sci*. 2018;19(5):1310.
8. Carninci P, Kasukawa T, Katayama S, et al. The transcriptional landscape of the mammalian genome. *Science*. 2005;309:1559-1563.
9. Anastasiadou E, Jacob LS, Slack FJ. Non-coding RNA networks in cancer. *Nat Rev Cancer*. 2018;18:5-18.
10. Kwok ZH, Tay Y. Long noncoding RNAs: links between human health and disease. *Biochem Soc Trans*. 2017;45:805-812.
11. Guttman M, Rinn JL. Modular regulatory principles of large non-coding RNAs. *Nature*. 2012;482:339-346.
12. Beermann J, Piccoli MT, Viereck J, Thum T. Non-coding RNAs in development and disease: background, mechanisms, and therapeutic approaches. *Physiol Rev*. 2016;96:1297-1325.
13. Rinn JL, Chang HY. Genome regulation by long noncoding RNAs. *Annu Rev Biochem*. 2012;81:145-166.
14. Bartel DP. Metazoan microRNAs. *Cell*. 2018;173:20-51.
15. Bracken CP, Scott HS, Goodall GJ. A network-biology perspective of microRNA function and dysfunction in cancer. *Nat Rev Genet*. 2016;17:719-732.
16. Svoronos AA, Engelman DM, Slack FJ. OncomiR or tumor suppressor? The duplicity of microRNAs in cancer. *Cancer Res*. 2016;76:3666-3670.

17. Bartel DP. MicroRNAs: target recognition and regulatory functions. *Cell*. 2009;136:215-233.
18. Salmena L, Poliseno L, Tay Y, Kats L, Pandolfi PP. A ceRNA hypothesis: the Rosetta Stone of a hidden RNA language? *Cell*. 2011;146:353-358.
19. Yang XZ, Cheng TT, He QJ, et al. LINC01133 as ceRNA inhibits gastric cancer progression by sponging miR-106a-3p to regulate APC expression and the Wnt/β-catenin pathway. *Mol Cancer*. 2018;17(1):126.
20. Kong X, Duan Y, Sang Y, Li Y. LncRNA-CDC6 promotes breast cancer progression and function as ceRNA to target CDC6 by sponging microRNA-215. *J Cell Physiol*. 2019;234:9105-9117.
21. Chen DL, Lu YX, Zhang JX, et al. Long non-coding RNA UICLM promotes colorectal cancer liver metastasis by acting as a ceRNA for microRNA-215 to regulate ZEB2 expression. *Theranostics*. 2017;7:4836-4849.
22. Akhtar M, Al-Bozom IA, Al Hussain T. Papillary renal cell carcinoma (PRCC): An update. *Adv Anat Pathol*. 2019;26:124-132.
23. Yang F, Song Y, Ge L, Zhao G, Liu C, Ma L. Long non-coding RNAs as prognostic biomarkers in papillary renal cell carcinoma. *Oncol Lett*. 2019;18:3691-3697.
24. Kallen AN, Zhou XB, Xu J, et al. The imprinted H19 lncRNA antagonizes let-7 microRNAs. *Mol Cell*. 2013;52:101-112.
25. Rutnam ZJ, Du WW, Yang W, Yang X, Yang BB. The pseudogene TUSC2P promotes TUSC2 function by binding multiple microRNAs. *Nat Commun*. 2014;5:2914.
26. Chen Y, He J, Su C, et al. LINC00461 affects the survival of patients with renal cell carcinoma by acting as a competing endogenous RNA for microRNA-942. *Oncol Rep*. 2019;42:1924-1934.
27. Yang K, Lu XF, Luo PC. Identification of six potentially long noncoding RNAs as biomarkers involved competitive endogenous RNA in clear cell renal cell carcinoma. *Biomed Res Int*. 2018;2018:9303486.
28. Huang C, Yuan N, Wu L, et al. An integrated analysis for long noncoding RNAs and microRNAs with the mediated competing endogenous RNA network in papillary renal cell carcinoma. *Onco Targets Ther*. 2017;10:4037-4050.
29. Luo Q, Cui M, Deng Q, Liu J. Comprehensive analysis of differentially expressed profiles and reconstruction of a competing endogenous RNA network in papillary renal cell carcinoma. *Mol Med Rep*. 2019;19:4685-4696.
30. Zhu X, Tan J, Liang Z, Zhou M. Comprehensive analysis of competing endogenous RNA network and 3-mRNA signature predicting survival in papillary renal cell cancer. *Medicine (Baltimore)*. 2019;98:e16672.
31. Xouri G, Lygerou Z, Nishitani H, Pachnis V, Nurse P, Taraviras S. Cdt1 and geminin are down-regulated upon cell cycle exit and are over-expressed in cancer-derived cell lines. *Eur J Biochem*. 2004;271:3368-3378.
32. Petropoulou C, Kotantaki P, Karamitros D, Taraviras S. Cdt1 and Geminin in cancer: markers or triggers of malignant transformation? *Front Biosci*. 2008;13:4485-4494.
33. Caillat C, Perrakis A. Cdt1 and geminin in DNA replication initiation. *Subcell Biochem*. 2012;62:71-87.
34. Fan Z, Wang Z, Chen W, Cao Z, Li Y. Association between the CYP11 family and six cancer types. *Oncol Lett*. 2016;12:35-40.
35. Lai CY, Xu Y, Yu GS, et al. Engrailed-2 might play an anti-oncogenic role in clear-cell renal cell carcinoma. *J Mol Histol*. 2016;47:229-237.
36. Wright CM, Savarimuthu Francis SM, Tan ME, et al. MS4A1 dysregulation in asbestos-related lung squamous cell carcinoma is due to CD20 stromal lymphocyte expression. *PLoS One*. 2012;7:e34943.
37. Yamakawa T, Miyata S, Ogawa N, et al. cDNA cloning of a novel trypsin inhibitor with similarity to pathogenesis-related proteins, and its frequent expression in human brain cancer cells. *Biochim Biophys Acta*. 1998;1395:202-208.
38. Jiang Y, Zheng X, Jiao D, et al. Peptidase inhibitor 15 as a novel blood diagnostic marker for cholangiocarcinoma. *EBioMedicine*. 2019;40:422-431.
39. O'Shea JJ, Schwartz DM, Villarino AV, Gadina M, McInnes IB, Laurence A. The JAK-STAT pathway: impact on human disease and therapeutic intervention. *Annu Rev Med*. 2015;66:311-328.
40. Taciak B, Pruszynska I, Kiraga L, Bialasek M, Krol M. Wnt signaling pathway in development and cancer. *J Physiol Pharmacol*. 2018;69(2).